

Current Status of Nucleon Decay Searches with Super-Kamiokande

Brett Viren for the Super-Kamiokande Collaboration
State University of New York at Stony Brook

Evidence for Nucleon Decay has yet to be observed. Current results from the observation of a 45 kton-year exposure of Super-Kamiokande and lifetime limits for nucleons to decay via lepton + pion, lepton + eta and lepton + kaon modes are presented.

I. MOTIVATION

In the Standard Model it is assumed that the proton is completely stable because there are no lighter products to which the proton could decay without violating baryon number conservation. However, the requirement for an interaction to conserve baryon number is not backed up by any symmetry in the Standard Model. If baryon number conservation is an incorrect assumption, then there are avenues for protons (as well as neutrons which are in stable nuclei) to decay.

Furthermore, most theories which go beyond the Standard Model allow or in most cases require, protons to be unstable at some level. One of the constraints on such theories is to predict a proton lifetime which does not contradict current measured lifetime limits. Experimental limits on the proton lifetime can kill or constrain such theories beyond the Standard Model. Furthermore, the actual observation of proton decay would help open the door to new physics as well as give answers to the ultimate state of matter in our universe in the far and distant future.

One of the primary goals of the Super-Kamiokande experiment is to search for proton (and neutron) decay. The results of such searches performed thus far are presented.

II. Super-Kamiokande DETECTOR

Super-Kamiokande is a ring imaging water Cherenkov detector containing 50 ktons of ultra pure water held in a cylindrical stainless steel tank 1 km underground in a mine in the Japanese alps. The sensitive volume of water is split into two parts. The 2 m thick outer detector is viewed with 1885 20 cm diameter photomultiplier tubes (PMTs) and acts as a veto shield to tag incoming cosmic ray muons. It completely surrounds and is optically separated from the 33 m diameter, 36 m high inner detector which is the primary sensitive volume. The inner detector contains 32.5 ktons of water and is viewed by 11146 inward pointing 50 cm diameter PMTs, giving a 40% photocathode coverage.

When relativistic charged particles pass through the water they emit Cherenkov light at an angle of about 42° from the particles direction of travel. When this cone of light intersects with the detector wall it is possible to image it as a ring. By measuring the charge produced in each PMT and the time at which it is collected, it is possible to reconstruct the position and energy of the event as well as the number, identity and momenta of the individual charged particles in the event.

III. ATMOSPHERIC NEUTRINO BACKGROUND

Many very exciting results have come from studying what is thought to be merely the background to proton decay events. Of particular note is the continued confirmation [1,2] of the atmospheric neutrino problem as well as finding evidence of massive neutrinos [3] as the only conceivable solution.

For proton decay searches there are three classes of atmospheric neutrino background events. The first is that of inelastic charged current events, $\nu N \rightarrow N'\{e, \mu\} + n\pi$, where a neutrino interacts with a nucleon in the water and

produces a visible lepton and some number of pions. This can mimic proton decay modes such as $p \rightarrow e^+\pi^0$.¹ The second class is neutral current pion production, $\nu N \rightarrow \nu N' + n\pi$, the only visible products of which are pions. This is a background to, for example, $n \rightarrow \bar{\nu}\eta$.² Finally, there is the mainstay of the atmospheric neutrino group, single ring quasi elastic charged current, $\nu N \rightarrow N'\{\mu, e\}$, events which can look like, for example, $p \rightarrow \bar{\nu}K^+$ decays.³

IV. THE $p \rightarrow e^+\pi^0$ MODE

The first mode discussed is $p \rightarrow e^+\pi^0$. Since this is one of the simplest modes it serves well as a general example of proton decay searches with Super-Kamiokande and will be discussed in some detail.

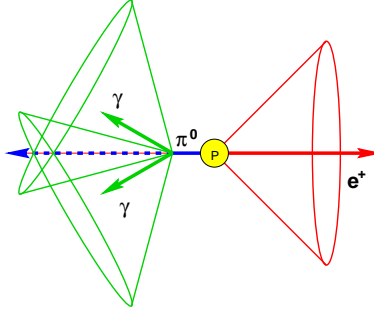


FIG. 1. Idealized $p \rightarrow e^+\pi^0$ decay in Super-Kamiokande.

Figure 1 shows a cartoon of an ideal $p \rightarrow e^+\pi^0$ decay. Here, the positron, e^+ and neutral pion, π^0 , exit the decay region in opposite directions. The positron initiates an electromagnetic shower leading to a single isolated ring. The π^0 will almost immediately decay to two photons which will go on to initiate showers creating two, usually overlapping, rings.

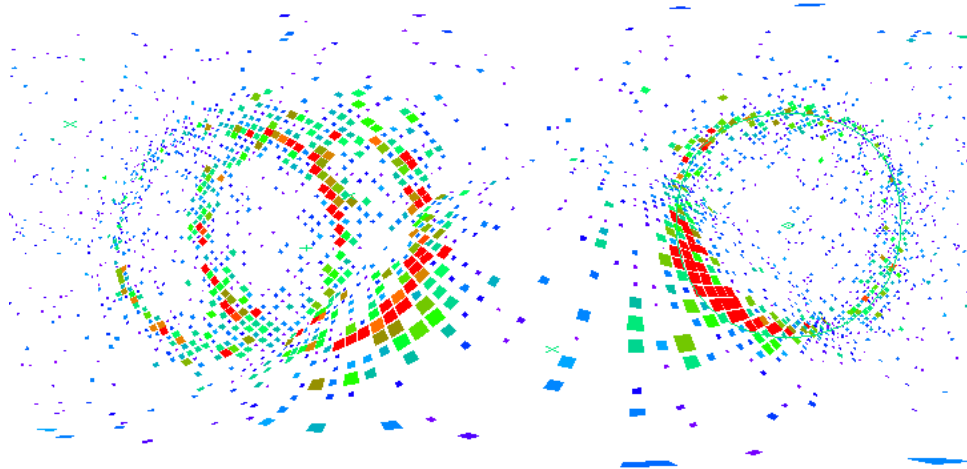


FIG. 2. $p \rightarrow e^+\pi^0$ MC event display.

In Super-Kamiokande, such an ideal event might look like Fig. 2. This event was generated with a detailed $p \rightarrow e^+\pi^0$ event and detector Monte Carlo (MC) simulation. In this figure, the PMTs are plotted as a function of

¹Thesis students: M. Shiozawa, B. Viren

²Thesis student: J. Kameda

³Thesis students: M. Earl, Y. Hayato

$\cos \theta$ *vs.* ϕ as viewed from the event vertex and are represented by squares, colored by amount of collected charge (red is more, blue is less) and sized to show distance from the event vertex. The fuzzy outer edges of the rings indicate an electromagnetic showering type of ring. Had the positron been replaced with a muon the single isolated ring would have a sharp, distinct edge.

In general, real $p \rightarrow e^+\pi^0$ events will differ from this ideal picture above because the pion can scatter or be absorbed entirely before it exits the nucleus. In addition the nuclear proton can have some momentum due to Fermi motion. These two effects, pion-nucleon interaction and Fermi motion, result in a breaking of the balance of reconstructed momentum. In addition, the pion can decay asymmetrically where one photon takes more than half of the pion's energy leaving the second photon to create a faint or even completely invisible ring. These effects, plus energy resolution and systematic uncertainties are considered when choosing the cuts to isolate possible decay events from their background.

The same reduction of the 5 Hz raw (high energy) trigger rate at Super-Kamiokande to the so called ‘‘contained event sample’’ (for more information see [1,4]) is used to find candidates for proton decay events as well as atmospheric neutrino events. From this reduced data sample, selection criteria unique to each search are applied to reduce the atmospheric background while keeping the efficiency to find a particular decay mode high.

For the $p \rightarrow e^+\pi^0$ mode, the selection criteria are as follows: (A) $6000 < Q_{tot} < 9500$ photoelectrons (PEs), (B) 2 or 3 e-like (showering type) rings, (C) if 3 rings: $85 < M_{inv,\pi^0} < 185 \text{ MeV}/c^2$, (D) no decay electrons, (E) $800 \text{ MeV}/c^2 < M_{inv,tot} < 1050 \text{ MeV}/c^2$, and (F) $P_{tot} = \left| \sum \vec{P}_i \right| < 250 \text{ MeV}/c$. The criterion (A) corresponds to a loose energy cut which reduces the background with out much computation needed. As stated above, it is possible for one of the photons to be invisible, for which (B) allows. If there are 3 rings criterion (C) requires that 2 of the rings reconstruct to give a π^0 mass. Since there are no muons nor charged pions expected, no decay electrons should be found and any events which have them will be cut by (D). Finally (E) requires the total invariant mass to be near that of the proton and (F) requires the total reconstructed momentum (magnitude of the vector sum of all individual momenta) to be below the Fermi momentum for ^{16}O .

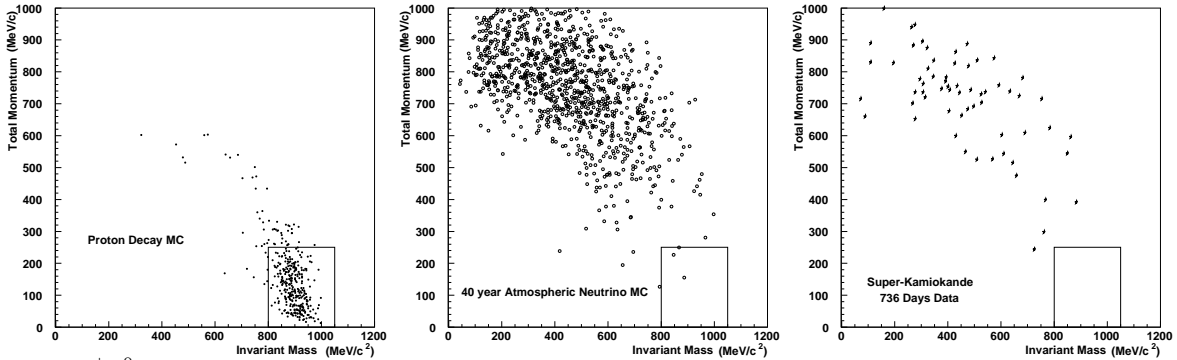


FIG. 3. $p \rightarrow e^+\pi^0$ mode. Distributions of events in total reconstructed momentum *vs.* total invariant mass for (a) proton decay MC, (b) atmospheric neutrino MC, and (c) data.

Figure 3 shows distributions of $p \rightarrow e^+\pi^0$ MC, atmospheric MC, and data in reconstructed momentum *vs.* invariant mass after criteria (A)-(D) have been applied. Criteria (E) and (F) shown by the box.

When these criteria are applied to 45 kton-years (736 days) of data we find no candidate events. Using atmospheric neutrino background MC equivalent to 40 years of data taking it is estimated that 0.2 background events are expected in the data. From MC simulations of $p \rightarrow e^+\pi^0$ events, the efficiency to select any $p \rightarrow e^+\pi^0$ events in the data sample is 44%. This gives a limit on the proton lifetime divided by $p \rightarrow e^+\pi^0$ branching ratio (partial limit) of $\tau/B_{p \rightarrow e^+\pi^0} > 2.9 \times 10^{33}$ years (90% CL).

V. THE $p \rightarrow \mu^+ \pi^0$ MODE

The $p \rightarrow \mu^+ \pi^0$ mode is very similar to the $p \rightarrow e^+ \pi^0$ mode. The only difference is to replace (A), (B) and (D) above with: (A) $5000 < Q_{tot} < 7800$ PE, (B) 1 μ -like (non-showering) and 1 or 2 e-like rings, and (D) 1 decay electron, respectively. The region defined by criterion (A) is lower than in the above case because a muon is more massive than a positron and will go below Cherenkov threshold sooner, thus emitting less light. The other two differences are also due to having a muon in the final state instead of a positron.

When these criteria are applied, no decay candidates are found in the data. It is estimated 0.1 background events should exist and a selection efficiency of 35% is obtained. The resulting partial limit is $\tau/B_{p \rightarrow \mu^+ \pi^0} > 2.3 \times 10^{33}$ years (90% CL).

VI. THE η MODES

Variations on the above two modes are found by replacing the neutral pion by an eta particle decaying to two γ s. This gives the modes, $p \rightarrow e^+ \eta$, $p \rightarrow \mu^+ \eta$, and $n \rightarrow \bar{\nu} \eta$.

All selection criteria are then very similar to the two previous modes except for (B) which is tightened up to only allow three ring events (except for $n \rightarrow \bar{\nu} \eta$ which requires exactly two) and (D) which requires the eta invariant mass to be reconstructed in the region $470 < M_{inv,\eta} < 610$ MeV/c².

The $p \rightarrow e^+ \eta$ search results in no candidate events on top of an expected background of 0.3 events, a selection efficiency of 17% and a partial lifetime limit of $\tau/B_{p \rightarrow e^+ \eta; \eta \rightarrow \gamma\gamma} > 1.1 \times 10^{33}$ years (90% CL).

For $p \rightarrow \mu^+ \eta$, no background is expected and no candidate events are found. The selection efficiency is 12% and the partial lifetime limit is $\tau/B_{p \rightarrow \mu^+ \eta; \eta \rightarrow \gamma\gamma} > 0.78 \times 10^{33}$ years (90% CL)

Finally, the $n \rightarrow \bar{\nu} \eta$ search finds 5 candidates consistent with the 9 expected background events and a selection efficiency of 21%. The partial limit for this mode is $\tau/B_{n \rightarrow \bar{\nu} \eta; \eta \rightarrow \gamma\gamma} > 0.56 \times 10^{33}$ years (90% CL).

VII. THE $p \rightarrow \bar{\nu} K^+$ MODES



FIG. 4. $p \rightarrow \bar{\nu} K^+$ mode, $K^+ \rightarrow \pi^+ \pi^0$ and $K^+ \rightarrow \mu^+ \nu_\mu$ branches.

Super-Kamiokande searches for the $p \rightarrow \bar{\nu} K^+$ mode [5] by looking for the products from the two primary branches of the K^+ decay. These are pictured in Fig. 4. In the $K^+ \rightarrow \mu^+ \nu_\mu$ case, when the decaying proton is in the ¹⁶O, the nucleus will be left as an excited ¹⁵N. Upon de-excitation, a prompt 6.3 MeV photon will be emitted. So this second branch has two independent searches: one in which the signature of this prompt photon is required and one in which it is explicitly absent. Unlike the other modes presented, the $p \rightarrow \bar{\nu} K^+$ search has been done with data from only 33 kton-years (535 days) of exposure.

The criteria for the $p \rightarrow \bar{\nu} K^+$; $K^+ \rightarrow \pi^+ \pi^0$ search are as follows: (A) 2 e-like rings, (B) 1 decay electron, (C) $85 < M_{inv,\pi^0} < 185$ MeV/c², (D) $175 < P_{\pi^0} < 250$ MeV/c, (E) $40 < Q_{\pi^+} < 100$ PE. The π^+ is very close to Cherenkov threshold and is expected to only produce a small amount of light as in (E). Since this is not enough to produce an identifiable ring only the rings from the 2 photons from the decay of the π^0 are required in (A). These photons must reconstruct to an invariant mass in the range defined by (C) as well as a momentum range defined in (D).

Figure 5 shows the event distributions in Q_{π^+} vs. π^0 momentum for proton decay MC, atmospheric neutrino MC and data after criteria (A) through (C). Criteria (D) and (E) are represented by the box.

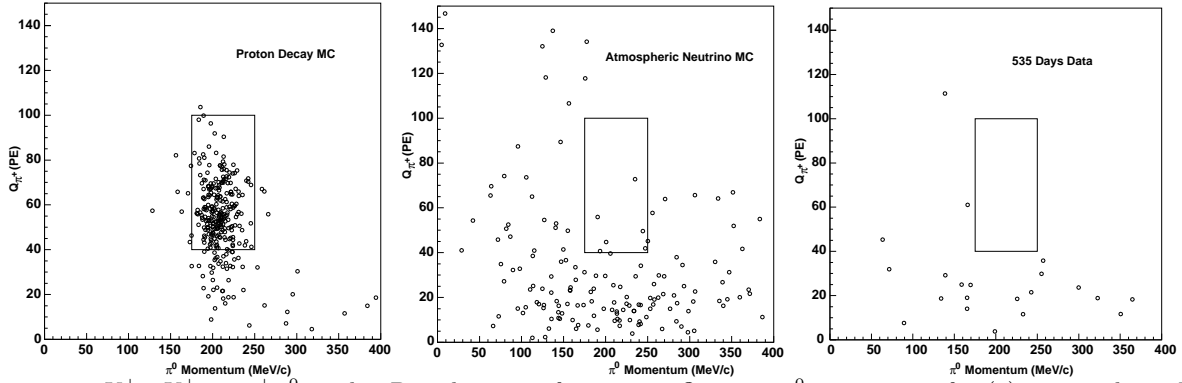


FIG. 5. $p \rightarrow \bar{\nu}K^+$; $K^+ \rightarrow \pi^+\pi^0$ mode. Distributions of events in Q_{π^+} vs. π^0 momentum for (a) proton decay MC, (b) atmospheric neutrino MC, and (c) data.

No candidates are found and 0.7 background events are expected. The selection efficiency is 6.5%, giving a partial lifetime limit of $\tau/B_{p \rightarrow \bar{\nu}K^+; K^+ \rightarrow \pi^+\pi^0} > 3.1 \times 10^{32}$ years (90% CL).

When searching for the $p \rightarrow \bar{\nu}K^+$; $K^+ \rightarrow \mu^+\nu_\mu$ with a 6.3 MeV prompt photon search the following criteria are required: (A) 1 μ -like ring, (B) 1 decay electron, (C) $215 < P_\mu < 260$ MeV/c, and (D) $N_{PMT} > 7$; $12 < t_{PMT} < 120$ ns before μ signal. The only particle giving a visible ring is the mono-energetic muon. Criteria (A-C) select for that. In criterion (D), t_{PMT} is the time a PMT was hit subtracted by the time it would take a photon to get directly from the fit event vertex to the PMT (so called “time minus time of flight” or “timing residual”). This requirement to have a significant number of hit PMTs within 1 to 10 kaon lifetimes is illustrated in Fig. 6.

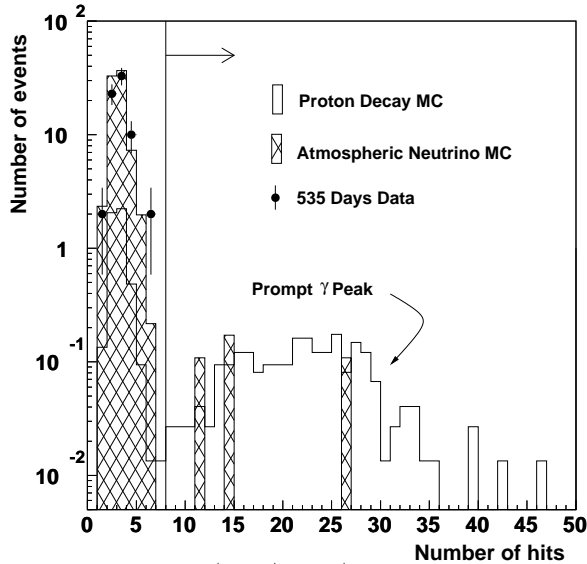


FIG. 6. $p \rightarrow \bar{\nu}K^+$; $K^+ \rightarrow \mu^+\nu_\mu$ mode with prompt γ signature. The atmospheric neutrino MC (hatched histogram) and proton decay MC (empty histogram) has been normalized to the data (dots).

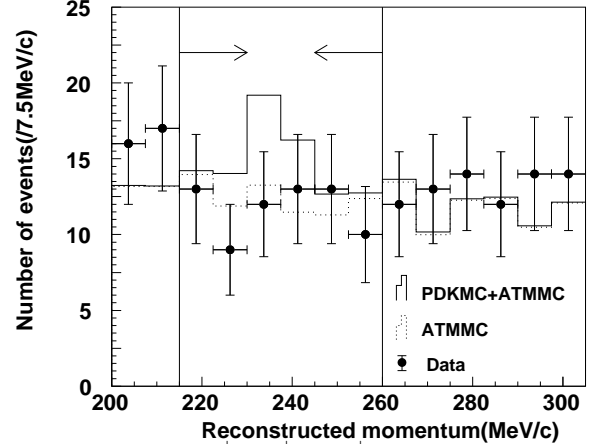


FIG. 7. $p \rightarrow \bar{\nu}K^+$; $K^+ \rightarrow \mu^+\nu_\mu$ with out prompt γ signature. The solid PDKMC+ATMMC histogram shows the atmospheric neutrino MC plus the proton decay MC assuming a proton lifetime that of the found 90% CL. The dotted ATMMC histogram is just the atmospheric neutrino MC normalized to the data which are the dots.

This search has an efficiency of 4.4%, finds no candidates on an estimated background of 0.4 events, and sets a limit of $\tau/B_{p \rightarrow \bar{\nu}K^+; (\gamma)K^+ \rightarrow (\gamma)\mu^+\nu_\mu} > 2.1 \times 10^{32}$ years (90% CL).

The complimentary case where no prompt gamma is allowed has the same criteria as the prompt gamma case except for the last: (D) $N_{PMT} \leq 7$; $12 < t_{PMT} < 120$ ns before μ signal. Since this allows a significant amount of

background to survive the selection criteria the limit is set by fitting for an excess of proton decay events above the atmospheric neutrino background in the reconstructed momentum spectrum. This is shown in Fig. 7. What is found is that, if anything, the data fluctuates downward in the region of expected muon momentum.

In this region, 70 candidate events are found which is consistent with the 74.5 events expected from atmospheric neutrinos. With an efficiency of 40% a limit of $\tau/B_{p \rightarrow \bar{\nu} K^+; (\gamma) K^+ \rightarrow (\gamma) \mu^+ \nu_\mu} > 3.3 \times 10^{32}$ years (90% CL) is found.

The combined limit for these three topologies is $\tau/B_{p \rightarrow \bar{\nu} K^+; K^+ \rightarrow \mu^+ \nu_\mu} > 6.8 \times 10^{32}$ years (90% CL).

VIII. THE $p \rightarrow \mu^+ K^0$ MODE

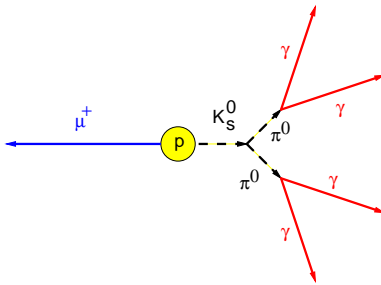


FIG. 8. $p \rightarrow \mu^+ K^0$ mode.

The search for proton decay via $p \rightarrow \mu^+ K^0$ so far relies on $K_s^0 \rightarrow \pi^0 \pi^0 \rightarrow \gamma \gamma \gamma \gamma$ decay branch of the kaon. The selection criteria for this are: (A) 1 μ -like and 2 or more e-like rings, (B) 1 or less decay electron, (C) $400 < M_{inv, K^0} < 600$ MeV/c², (D) $150 < P_\mu < 400$ MeV/c, (E) $750 < M_{inv, tot} < 1000$ MeV/c², and (F) $P_{tot} < 300$ MeV/c. Because it is possible for one photon from each pion to be missed, only 2 are required in (A) in order to preserve a high efficiency. Using all e-like rings, a reconstructed K^0 mass is required in (C). The reconstructed muon momentum should be a discrete value smeared by Fermi motion and energy resolution as is required in (D). Finally, (E) and (F) require total invariant mass near proton rest mass and total reconstructed momentum to be less than the Fermi momentum.

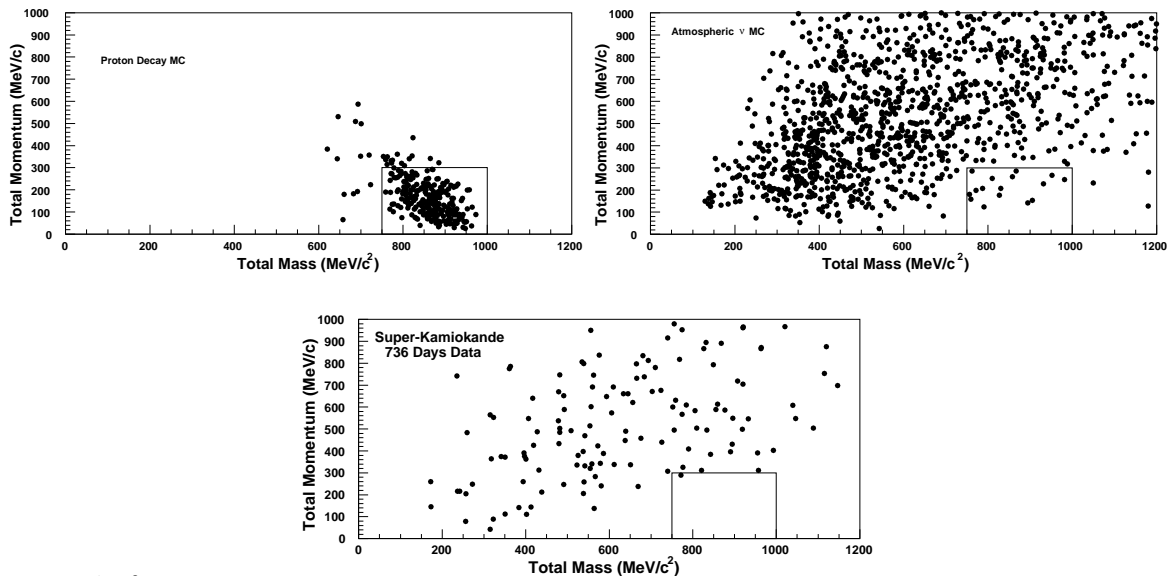


FIG. 9. $p \rightarrow \mu^+ K^0$ mode. Distributions of events in total reconstructed momentum *vs.* total invariant mass for (a) proton decay MC, (b) atmospheric ν MC and (c) data. The boxes represent criteria (E) and (F).

Figure 9 shows the event distributions in total momentum *vs.* total invariant mass for proton decay MC, atmospheric neutrino MC and the data for events which pass criteria (A) and (B). The boxes represent criteria (E) and (F). The

single data event which is inside the box is far outside the requirements of (C) and (D) and so is not a valid candidate.

This search was done on 45 kton-years of data and has a 6.1% efficiency. No candidates were found and 0.65 background events were expected. The resulting limit is $\tau/B_{p \rightarrow \mu^+ K^0} > 4.0 \times 10^{32}$ years (90% CL).

IX. SUMMARY OF SEARCHES

The current Super-Kamiokande nucleon decay results are summarized in Table I. As a comparison, limits collected in PDG 1998 [6] are also included. Finally, although the best limits have been set by large water Cherenkov experiments, iron calorimeters offer a complementary search with tracking sensitivity to kaons and low momentum pions and muons. Recent results from the Soudan 2 experiment were also presented and are listed below.

TABLE I. Summary of nucleon decay searches. All limits are in units of 10^{32} years and are at 90% confidence level.

Mode	Super-Kamiokande	PDG 1998	Soudan 2
$p \rightarrow e^+ \pi^0$	29	5.5	–
$p \rightarrow \mu^+ \pi^0$	23	2.7	–
$p \rightarrow e^+ \eta$	11	1.4	0.70
$p \rightarrow \mu^+ \eta$	7.8	0.69	0.78
$n \rightarrow \bar{\nu} \eta$	5.6	0.54	0.64
$p \rightarrow \bar{\nu} K^+$	6.8	1.0	0.78
$p \rightarrow e^+ K^0$	–	0.76	0.72
$p \rightarrow \mu^+ K^0$	4.0	0.64	1.04
$n \rightarrow \bar{\nu} K_s^0$	–	0.86	0.62

-
- [1] Y. Fukuda *et al.*, Phys. Lett. **B433**, 9-18 (1998).
 - [2] Y. Fukuda *et al.*, Phys. Lett. B **436**, 33-41 (1998).
 - [3] Y. Fukuda *et al.*, Phys. Rev. Lett. **81**, 1562-1567 (1998).
 - [4] M. Shiozawa *et al.*, Phys. Rev. Lett. **81** 3319-3323 (1998).
 - [5] Y. Hayato *et al.*, Submitted to Phys. Rev. Lett.
 - [6] C. Caso *et al.*, The European Physical Journal **C3** 614-619 (1998).